Towards laser-induced fluorescence of nitric oxide in detonation

Karl P. Chatelain[1,2], **Samir B. Rojas Chavez**[1,2], **João Vargas**[1,2], **Deanna A. Lacoste**[1,2]

[1] Mechanical Engineering Program, Physical Science and Engineering Division, King Abdullah University of Science and Technology (KAUST), Thuwal 23955-6900, Kingdom of Saudi Arabia

[2] KAUST Clean Combustion Research Center (CCRC), King Abdullah University of Science and Technology

1 Introduction

Since the discovery of detonation, many studies were performed to characterize the propagation regime (stable vs oscillatory mode) and characteristic parameters (e.g., cell size or critical parameters) of detonations in different experimental configurations, range of conditions, and fuels. Among all these studies, only a limited number of laser diagnostics were employed, e.g, laser-induced fluorescence of OH radical (OH-PLIF) or Rayleigh scattering, for two-dimensional (2D) qualitative or quantitative characterization of the detonation front, as compared to work done on subsonic flames. A few research groups characterized the detonation structure with the OH-PLIF technique [1, 2]. Despite the limitations of the OH-PLIF diagnostic, notably the strong laser absorption and the limited information far from the detonation front, these measurements enabled a better understanding of the detonation structure in various conditions. Recent studies employing the OH-PLIF technique [3, 4] evidenced that using a transverse laser orientation or selecting different excitation strategies can suppress part of these limitations. In addition to a better usage of the current diagnostics, employing new laser diagnostics seem to be a promising way towards more phenomenological comprehension of H_2-air detonation. Despite the extensive usage of the laser-induced fluorescence of nitric oxide (NO-LIF) technique in flame diagnostics or hypersonic flows, there is no prior usage of NO-LIF in detonation.

This study aims to numerically and experimentally evaluate the capabilities of the NO-LIF diagnostic for characterizing H_2-air detonation. This study focuses on extending the capabilities of our in-house spectroscopic code (KAT-LIF) to perform NO-LIF simulations. A validation of the code is then proposed based on comparisons with experimental and numerical data obtained for (i) a stoichiometric CH_4-air flame, and (ii) a stoichiometric H_2-air detonation.

2 Numerical method

2.1 Presentation of KAT-LIF

In [3], we developed and validated an in-house spectroscopic code called KAT-LIF. The code was previously employed to simulate the evolution of the spectrally-resolved OH-LIF intensity along the beam path for a set of user-specified parameters (e.g., laser parameters, mixture composition, and thermodynamic conditions). For OH-LIF simulations, the code utilizes the spectroscopic parameters of the OH transitions available in HITRAN [5], as previously reported in [2–4]. Also, KAT-LIF has several built-in functions that makes its usage more suitable compared to other existing tools [6–8]. For example, KAT-LIF's input is one-dimensional (1D) and some simulation parameters are calculated within the code based on both the mixture composition and the thermodynamic conditions (e.g., shifting and broadening of the lines, quenching, laser self-absorption). Both features make the simulation of high spatially resolved systems, such as detonations, more practical to simulate compared to point simulation softwares.

In this section, we present the three main updates of KAT-LIF enabling the NO-LIF simulations. These

updates were focused on: a) building the NO database, b) adding the NO quenching calculation, and c) adding the NO pressure shifts.

a) Building the NO database To the best of the authors' knowledge, none of typical spectroscopic databases reports detailed list of rovibrationaly-resolved NO(A-X) transitions with their associated spectroscopic parameters required in KAT-LIF simulations, namely: the line position ν (in m^{-1}), the Einstein-A coefficients A (in s^{-1}), the spectral line strength (also called spectral line intensity in HITRAN) at 296 K S_{ref} (in $\mathrm{m}^{-1}/(\mathrm{molecule} \cdot \mathrm{m}^{-2})$), the upper ($g'$, unitless) and lower ($g''$, unitless) state degeneracies (also called the statistical weights), and the lower-state energy of the transition E'' (also called $E0$). Note that the NO transitions currently reported in HITRAN/HITEMP belongs to the NO(X-X) transitions ($>>$ 250 nm) and are not of interest for the present NO-LIF application.
Thus, a NO(A-X) database was built according to the following procedure. The ν and A coefficients were directly obtained from LIFBASE [6]. E'' was obtained from simple energy conservation calculations using $E' = E'' + \nu$, where E' and E'' are the upper- and lower-state energy of the transition ν (in cm^{-1}). Note E' and E'' were rescaled by setting the lowest E'' to 0, as performed in HITRAN [5]. g' and g'' were obtained from the hyperfine calculation presented in [9], which gives for NO(A-X) transitions $g_{F1} = (2 \times (J^\star - 0.5) + 1) \times g_s$ and $g_{F2} = (2 \times (J^\star + 0.5) + 1) \times g_s$, where g_{F1} and g_{F2} are the degeneracy for F1 and F2 level; $J^\star$ corresponds to any upper (J') or lower (J'') rotational level; g_s corresponds to the state-dependent weight for NO provided in [9]. The line intensity was computed according to the equation presented in [2] by using the isotope abundance from [5] and the NO partition function from [10].
As a results, the generated NO(A-X) database includes more than 100 000 transitions from 1060623 to 5695552 m^{-1} ($\approx 176 - 943$ nm), among the following upper and lower vibrational levels $v' = 0 - 5$ and $v'' = 0 - 21$, and lower rotational quantum number $N'' = 0 - 80$. Note the database could be extended for NO(B-X), NO(C-X), and NO(D-X) transition by using an analogous procedure.

b) NO quenching calculation The collisional quenching rate of NO with other colliders i is computed with the following equation from Paul et al. [11].

$$Q = \frac{P}{kT}\left(\frac{8kT}{\pi m_{\mathrm{NO}}}\right)^{0.5} \sum x_i \left(1 + \frac{m_{\mathrm{NO}}}{m_i}\right)^{0.5} \sigma_{Qi} \tag{1}$$

where P and T are the pressure (in Pa) and temperature (in K), respectively; k is the Boltzmann constant (in J/K); m_{NO}, m_i, x_i, and σ_i are the mass of NO, the mass of the collider i, the mole fraction of i, and the collisional quenching cross-section of the collider i respectively; The temperature dependence of σ_i were obtained from Paul [11] for NO_2, N_2O, and NH; Tamura et al. [12] for H, H_2, OH, CH_4; Settersten et al. [13] for CO_2, CO, NO, C_2H_2; Settersten et al. [14] for O_2, H_2O, and N_2.

c) Line shift updates As performed for OH [4], the pressure shift of the NO transition lines is computed with Eq.2

$$\nu_s = \nu + P \sum_i x_i \delta_{i,T_{\mathrm{ref}}} \left(\frac{T_{\mathrm{ref}}}{T}\right)^{m_i} \tag{2}$$

where ν_s and ν are the shifted and the initial transitions (in m^{-1}); $\delta_{i,T_{\mathrm{ref}}}$ and m_i are the shift coefficient (in $\mathrm{m}^{-1}/\mathrm{atm}$) of the species i at the reference temperature (T_{ref}) and the temperature exponent (no unit), respectively. $\delta_{i,T_{\mathrm{ref}}}$ and m_i parameters were obtained from [15, 16] for N_2, Ar, H_2O, and O_2.

2.2 Steady detonation modeling

The Zel'dovich von Neumann Döring (ZND) simulations are performed with the shock module of Chemkin-Pro, as employed in [17, 18]. As demonstrated in [17], this reactor model has the same performance as the conventional steady detonation modeling tools. The reaction model of Mével et al. [19]

was employed for the ZND simulations of H_2-air mixtures. This model comprises 31 species and 193 reactions. The ZND simulation outputs were employed as an input of KAT-LIF to model the NO LIF signal evolution along the detonation. Figures 1a and 1b present the effect of the NO addition (without and with NO addition in open symbols and solid line, respectively) on the ZND profiles of a stoichiometric H_2-air detonation, initially at $P_1 = 10$ kPa and $T = 293$ K, for 100 ppm and 1000 ppm NO addition, respectively. As there is no effect of the NO addition on the main quantities (Temperature, pressure, and thermicity), the H_2-air-NO mixture can effectively be employed to characterize the H_2-air detonation. In addition, this NO quantity can be adjusted to improve the signal-to-noise ratio.

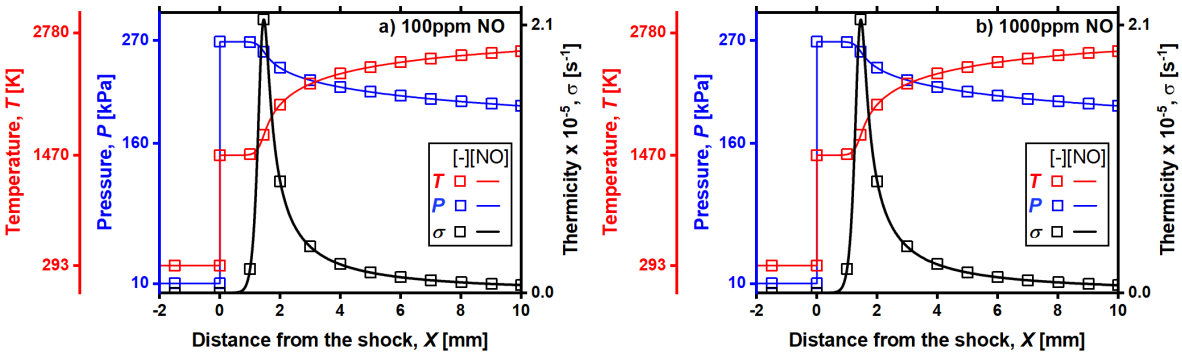

Figure 1: Effect of a 100 ppm (in a) and 1000 ppm (in b) NO addition on the temperature (in red), pressure (in blue), and thermicity (in black) profiles compared to a neat stoichiometric H_2-air detonation. The profiles without NO addition are in open symbols and the ones with NO are in solid lines. Conditions are $P_1 = 10$ kPa and $T = 293$ K.

2.3 Validation procedure

The updated KAT-LIF code was validated, experimentally, with new measurements and, numerically, by comparing the simulation results with already developped simulation tools, such as LIFBASE [6] and LIFSim [7]. Note that all the presented NO-LIF results consider a frontal laser orientation (i.e., laser propagating in the opposite direction of the detonation, see [4]) and the fluorescence is in the linear regime. The validation was performed in two steps. First, the evolution of fluorescence intensities in a stoichiometric methane-air flame, initially at $P = 101$ kPa and $T = 293$ K, was compared between KAT-LIF, LIFBASE, LIFSim, and experimental results for different laser excitation wavelengths in the (0,0) and (0,1) bands. Second, the evolution of the fluorescence intensity in a stoichiometric H_2-air detonation, initially at $P_1 = 10 - 20$ kPa and $T = 293$ K, was compared between KAT-LIF, LIFSim, and experimental results for a laser excitation wavelength at 225.120 nm, typically employed in flame diagnostics. Note the fluorescence intensity evolution in a detonation cannot be simulated with LIFBASE, due to the built-in autoscale. In addition to these validations, the lines positions between LIFSim and KAT-LIF were compared in both the (0,0) and (0,1) bands and presented an average error of 0.3 and 0.4 pm with a maximum error of 0.5 and 0.6 pm, respectively.

Experimentally, the same laser system, optical arrangement, optical detonation duct (ODD), and visualization system (i.e., camera, lens, and filter) as [20] were employed in this study. Also, the post processing procedure from [20] was followed to obtain the background- and chemiluminescence-corrected 1D NO-LIF profile. The noteworthy differences with [20] are: a 20-ns gate width was set on the camera and a 1000-ppm NO seeded laminar CH_4-air flame was employed in the slot burner for the laser scan.

3 Results and discussions

Laser scan validation Figures 2a and 2b present the fluorescence intensity evolution as a function of the laser excitation wavelength in the (0,0) and (0,1) bands, respectively. Figures 2a compares KAT-LIF, LIFSim, and experimental results obtained in the burned gases of a laminar premixed CH_4-air flame, initially at $T = 293$ K, $P = 101$ kPa, and $\phi = 1$. Note the flame was seeded with 1000 ppm of NO to ensure a satisfactory signal-to-noise ratio. Figures 2b compares KAT-LIF, LIFSim, and LIFBase results for the same conditions with a laser excitation wavelength in the (0,1) band. Note, only numerical validation of KAT-LIF was performed in the (0,1) band due to the experimental limitations of the Rhodamine 590 dye and the camera filter (Semrock LP02-224R) which cannot be employed for the (0,1) band. Figures 2a and 2b confirm the satisfactory agreement of the different simulations tools, among each other and with experimental results, at reproducing the fluorescence intensity evolution in atmospheric conditions ($P = 101$ kPa) and high temperature ($T \approx 2230$ K) for different laser excitation wavelengths. Also, these results indirectly validates the spectroscopic parameters calculated in NO(A-X) database.

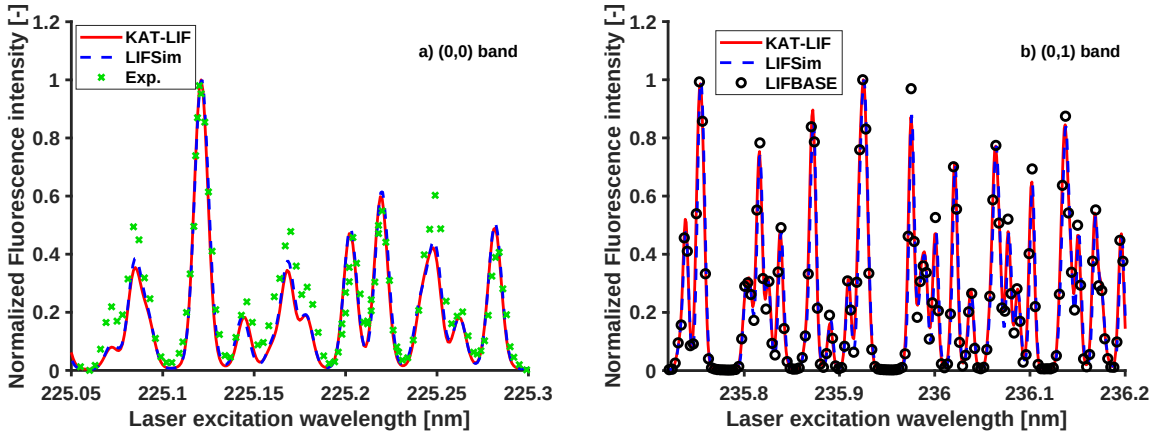

Figure 2: Fluorescence intensity evolution as a function of the laser excitation wavelength, including both experimental (Exp.) and simulation data (KAT-LIF, LIFSim,and LIFBASE), in the (0,0) and the (0,1) band in a and b, respectively. The conditions are: 8-pm FWHM laser width, $T = 2233$ K, $P = 101$ kPa, with the following major species: $x_{N_2} = 0.71$, $x_{CO_2} = 0.085$, and $x_{H_2O} = 0.18$. Note, LIFBASE results are not presented for clarity.

Detonation validation Figures 3a and 3b presents a numerical and an experimental validation of KAT-LIF, respectively. Figure 3a presents a tailored validation case, based on a modified H_2-air detonation profile, for which some input parameters were modified to facilitate the comparison between KAT-LIF and LIFSim simulation results. Figure 3b presents the differences between KAT-LIF and LIFSim simulation resulting from the same ZND profile as an input. Some noteworthy points about this tailored validation case (Fig.3a) are: (i) H_2 mole fraction was replaced by CH_4 in both codes, as H_2 cannot be specified in LIFSim; (ii) the NO concentration was fixed to 1000 ppm, as fixed in LIFSim. (iii) Doppler lineshift contribution was removed from KAT-LIF simulation, as Doppler lineshift is not considered in LIFSim; (iv) only CH_4, O_2, H_2O, and N_2 species are considered in both simulations to match the limited number of species in LIFSim. From Figure 3a, a satisfactory agreement between KAT-LIF and LIFSim is observed with an average and a maximum discrepancy of 7% and 17%, respectively.

Figure 3b compares the experimental (exp) and simulated (KAT-LIF and LIFSim) fluorescence signal evolution as a function of the distance behind the shock for a H_2-air detonation, initially at $P = 20$ kPa, $T = 293$ K, and a 225.120 nm laser excitation wavelength. Satisfactory agreement are obtained for both KAT-LIF and LIFSim at reproducing the experimental profile with an average error near 20% and 10%

in the reaction zone, respectively. Considering the variability of the LIF signal in the reaction zone, these low errors seem close to the experimental uncertainty of the NO-LIF experimental measurements. The differences in the NO-LIF profile between KAT-LIF and LIFSim can be mainly attributed to the simulations parameters, listed in (i)-(iv). Considering all the possible differences between the two codes (e.g., line positions or the broadening/shifting/quenching parameters), these small errors validate KAT-LIF developments and its NO(A-X) spectroscopic database.

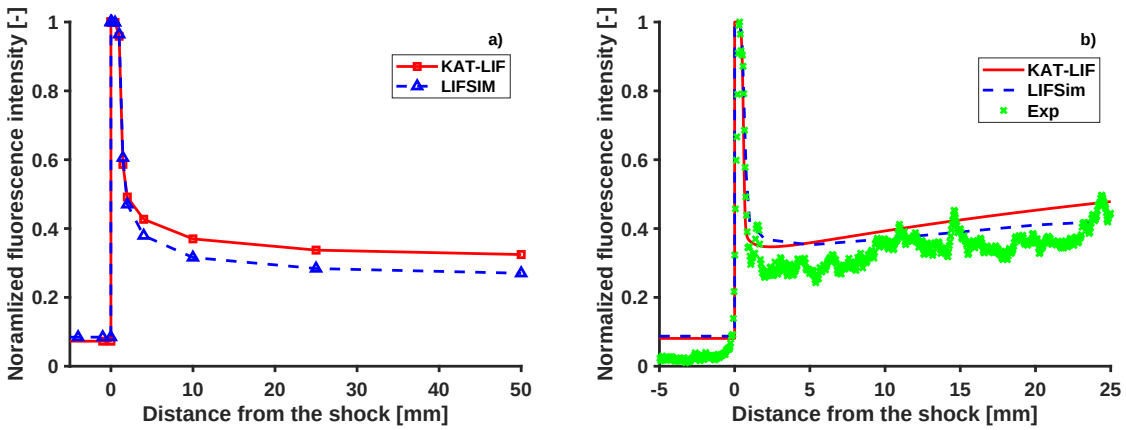

Figure 3: Normalized NO fluorescence intensity evolution as a function of the distance from the shock between KAT-LIF (red line) and LIFSim (blue symbol) in a tailored validation case (in a) and in a real H_2-air detonation (in b). Initial conditions are $P = 10$ and 20 kPa (in a and b, respectively) and $T = 293$ K. Note that H_2 is replaced by CH_4 in LIFSim simulations.

4 Conclusions

This study aimed at evaluating the capabilities of the NO-LIF diagnostic for characterizing H_2-air detonation. This objective was achieved in two steps. First, our in-house spectroscopic tool, KAT-LIF, was updated to perform NO-LIF simulations by notably developing a database of NO(A-X) transitions. Second, the validation of KAT-LIF was performed by comparing the simulation results with pre-existing simulation tools and experimental NO-LIF measurements in a laminar CH_4-air flame and H_2-air detonation. The validation results indicate: (i) the NO-LIF intensity evolution simulated by KAT-LIF was in agreement with experimental and other simulation tools (LIFBASE and LIFSim) results for different laser excitation wavelengths in a typical stoichiometric CH_4-air flame (atmospheric pressure and high temperature); (ii) both KAT-LIF and LIFSim were satisfactorily reproducing the LIF intensity evolution in a stoichiometric H_2-air detonation. The small discrepancy observed between both codes and the experimental profile are mainly attributed to the experimental uncertainties. (iii) Small numerical discrepancies, near 7%, were observed between KAT-LIF and LIFSim simulation results by using a tailored validation case. These marginal differences are related to small differences in both codes (e.g., line positions, quenching parameters, line shifting, or line broadening), which cannot be identified precisely. In addition, the present validation work evidenced the possibility to use the NO-LIF diagnostic in NO-seeded H_2-air detonation. Furthermore, our ZND simulation results revealed that small NO addition in the H_2-air mixture do not modify the detonation structure and, as such, this NO quantity can be adjusted to improve signal-to-noise ratio. Future work will focus on obtaining quantitative measurements in H_2-air detonation by using the NO-LIF technique, as presented in [20].

Acknowledgments

The research reported in this publication was supported by funding from King Abdullah University of Science and Technology (KAUST), under award number BAS/1/1396-01-01.

References

[1] Pintgen F, Eckett CA, Austin JM *et al.* (2003). Direct observations of reaction zone structure in propagating detonations. Combust. Flame 133(3):211.

[2] Mével R, Davidenko D, Austin JM et al. (2014). Application of a laser induced fluorescence model to the numerical simulation of detonation waves in hydrogen–oxygen–diluent mixtures. Int J Hydrog Energy 39(11):6044.

[3] Rojas Chavez SB, Chatelain KP, Guiberti TF *et al.* (2021). Effect of the excitation line on hydroxyl radical imaging by laser induced fluorescence in hydrogen detonations. Combust. Flame 229(3):111399.

[4] Chatelain KP, Mével R, Melguizo-Gavilanes J *et al.* (2020). Effect of Incident Laser Sheet Orientation on the OH-PLIF Imaging of Detonations. Shock Waves 30:689.

[5] Gordon IE, Rothman LS, Hill C. (2017). The HITRAN2016 Molecular Spectroscopic Database. J. Quant. Spectrosc. Radiat. Transfer 203:3.

[6] Luque J (1999) LIFBASE, Database and spectral simulation for diatomic molecules. SRI International Report 99.

[7] Bessler WG, Schulz C, Sick V *et al.* (2003). A versatile modeling tool for nitric oxide LIF spectra. Proceedings of the Third Joint Meeting of the US Sections of The Combustion Institute, Chicago, IL. Paper P105.

[8] Foo KK, Lamoureux N, Cessou A *et al.* (2020). The accuracy and precision of multi-line NO-LIF thermometry in a wide range of pressures and temperatures.J. Quant. Spectr. Rad. Transfer 255:107257

[9] Šimečková M, Jacquemart D, Rothman LS *et al.* (2006). Einstein A-coefficients and statistical weights for molecular absorption transitions in the HITRAN database. J. Quant. Spectrosc. Radiat. Transf. 98(1):130.

[10] Gamache RR, Roller C, Lopes E *et al.* (2017). Total internal partition sums for 166 isotopologues of 51 molecules important in planetary atmospheres: Application to HITRAN2016 and beyond. J. Quant. Spectrosc. Radiat. Transf. 203:70.

[11] Paul PH, Gray JA, Durant JL *et al.* (1994). Collisional quenching corrections for laser-induced fluorescence measurements of NO $A^2\Sigma^+$. AIAA J. 32(8):1670–1675.

[12] Tamura M, Berg PA, Harrington JE *et al.* (1998). Collisional Quenching of CH(A), OH(A), and NO(A) in Low Pressure Hydrocarbon Flames. Combust Flame 114 (3):502.

[13] Settersten TB, Patterson BD, Gray JA. (2006). Temperature- and species-dependent quenching of NO $A^2\Sigma^+(\nu' = 0)$ probed by two-photon laser-induced fluorescence using a picosecond laser. J. Chem. Phys. 124(23):234308.

[14] Settersten TB, Patterson BD, Humphries IV WH. (2009). Radiative lifetimes of NO $A^2\Sigma^+(\nu' = 0, 1, 2)$ and the electronic transition moment of the $A^2\Sigma^+ - X^2\Pi$ system, J. Chem. Phys. 131(10):104309.

[15] Chang AY, DiRosa MD, Hanson RK. (1992). Temperature dependence of collision broadening and shift in the NO A←X (0,0) band in the presence of argon and nitrogen. J. Quant. Spectrosc. Radiat. Transf. 47 (5):375.

[16] Di Rosa MD, Hanson RK. (1994). Collision broadening and shift of NO γ(0,0) absorption lines by O_2 and H_2O at high temperatures. J. Quant. Spectrosc. Radiat. Transf. 52(5):515.

[17] Chatelain KP, He Y, Mével R *et al.* (2021). Effect of the reactor model on steady detonation modeling. Shock Waves 31(4):323.

[18] Chi DJY, Chatelain KP, Lacoste DA. (2022). Evaluation of detailed reaction models for the modeling of double cellular structures in gaseous nitromethane detonation. AIAA Scitech Forum. American Institute of Aeronautics and Astronautics, San Diego, CA.

[19] Mével R, Javoy S, Lafosse F *et al.* (2009). Hydrogen–nitrous oxide delay times. Shock tube experimental study and kinetic modelling. Proc. Combust. Inst. 32(1):359.

[20] Rojas Chavez SB, Chatelain KP, Lacoste DA. (2022). Induction zone length measurements by laser-induced fluorescence of nitric oxide in hydrogen-air detonations. 39th International Symposium on Combustion, Vancouver. Accepted for presentation.